Available online at http://jprm.sms.edu.pk/
Journal of Prime Research in Mathematics, 22(1) (2026), 132–144

Journal of Prime Research in Mathematics

Mathematical Modeling and Numerical Simulation for Cellular Systems

Aymen Hadji[a], Ibtissem Hadji[b], Fatma Zohra Nouri[c,*]

[a] *Department of Pharmacy, University Mostefa Benboulaid, Batna2-Algeria*
[b] *Cardiology Service, Angoulême Hospital, Angoulême-France*
[c] *Mathematical Modeling and Numerical Simulation Research Laboratory, Faculty of Sciences, Badji Mokhtar University, P.O. Box 12, Annaba 23000-Algeria.*

Abstract

In this work, we are interested in modeling biological cell migration and proliferation. These models provide a mathematical framework to analyze and simulate the intricate dynamics of tumor growth, considering factors such as cell proliferation, angiogenesis, and interactions with the surrounding microenvironment. This can help to develop new therapies, design biomaterials, and engineer tissues for regenerative medicine. We are going to derive a simple mathematical model able to fulfill some requirements of observed biological experiments, such as travelling waves and sharp cell fronts. When the cell density is large enough, the continuous medium assumption is a good approximation and partial differential equations can be written. The well-posedness of the derived model is proved in the strong sense using semi-group theory and weak sense by Lax-Miligram theorem. The numerical study has been carried out by the use of finite element methods, using an adaptative meshing to control the motion of the complex cell-structure due to cell moving fronts. The obtained numerical results are shown to be efficient and qualitatively significant for biology cell research applications.

Keywords: Mathematical Modeling, Analysis and Well-Posedness, Stability & Simulation.
2020 MSC: 35J50, 65M60, 65N30, 65P99, 68Q80.

1. Introduction

Cell proliferation and migration are structural biological processes taking part in development, tissue repair, and disease progression. Proliferation refers to the increase in cell number through cell division, while migration is the movement of cells from one location to another. These mechanisms are often interrelated and can control and influence each other, for example:
* Tumor-macrophage interactions, often promoting cancer growth, angiogenesis (new blood vessel formation), metastasis (spread), and immunosuppression [21].

*Fatma Zohra Nouri
Email addresses: a.hadji@univ-batna2.dz (Aymen Hadji), ibtissem.hadji@ch-angouleme.fr (Ibtissem Hadji), fatma-zohra.nouri@univ-annaba.dz (Fatma Zohra Nouri)

Received : 30 September 2025*; Accepted:* 14 April 2026*; Published Online:* 03 May 2026

* Research uses Ag/MgO-water hybrid nanofluids to model heat transfer for potential cancer therapies (hyperthermia), which could focus thermal treatment on tumors while minimizing damage to healthy tissue [17].
The development of mathematical models plays a crucial role in exploring tumoral cell proliferation and migration, offering perceptions for cancer diagnosis and treatment. A large range of systems have been proposed by different authors to describe cancer cell proliferation, incorporating physical and environmental factors that influence tumor development, see for example [11], and often exploring adopted data bases [18] and [19].
These models mainly based on nonlinear ordinary differential equations (ODEs) and partial differential equations (PDEs), have been employed to be significantly studied from diverse viewpoints, surrounding aspects including but not limited to, we can mention well-posedness, analytical and numerical solution, see for example [6], [10], [12], [13] and [20].

Our work is motivated by the the Keller-Segel (K-S) model in conservation form, that takes into account cell diffusion, proliferation and propagation due to the presence of a chemoattractant. Many authors have used the K-S Model, for example [12] for autowaves detection, [3] to approach K-S Systems gradient flow and [4] to show how to predict therapies. However the basic K-S model cannot reproduce traveling waves or sharp cell moving fronts, which are observed by biological experiments. Hence adding new modeling terms to the equations is obviously necessary.

The novel contribution here, is to replace the (K-S) convection term $\nabla(a\rho\nabla c)$, where a is a constant, by $\nabla(f(\rho)\nabla c)$, with $f(\rho)$ a well-suited nonlinear function of the density ρ.
Our objective in this paper, seeks to identify $f(\rho)$, examines and evalutes the mathematical analysis of the derived model to prove its well posedness, and investigates its numerical discretication by a stable efficient scheme based on finite elements, that must be able to handle the effect of meshing within the moving phenomenon.

This paper is structured as follows: in section 2, we introduce the proposed model. In section 3, we discuss the mathematical analysis of the derived model, while section 4 is devoted to the numerical study. Section 5 covers the obtaibed results and comments and we finish with a section of concluding remarks.

2. Proposed Model

2.1. Requirements

Due to biological expectations [13, 18, 21] and mathematical properties [6, 11, 14], we are going to derive a mathematical model able to fulfill the following requirements.

1. Without proliferation and apoptosis (cell death), the number of cell has to be conserved, so migration phenomenon should be modeled by a conservation law.

2. Travelling waves and sharp cell fronts are observed in biological experiments. Thus this behaviour must be reproduced by the model.

3. Sometimes cell fronts reach a steady state, i.e. the cell fronts slow down and stop in finite time. This reveals a cell region with a boundary and this behaviour also has to be reproduced by the model.

4. Known biochemical factors like chemoattractant and chemorepellent agents are able to attract or repel biological cells.

5. Cell motility is the ability for a cell to move freely, generally with a brownian motion. From the macroscopic point of view, this is a diffusive phenomenon. If the diffusion is isotropic, then the diffusion operator is the Laplace operator.

6. There are biological regulation factors which limit the cell density up to a certain threshold.

To meet these properties and expectations, the function $f(\rho)$ of the convection term in our proposed modified K-S model must be chosen in a well-considered manner, which constitutes our primary goal in this work.

2.2. Mathematical Model

The Keller-Segel (K-S) system being the first step toward the understanding of how, during the evolution of species, the motion from uni-cellular organisms to more complex structure was achieved. So it can be used as a model taking into account the requirements in section 2.1, but cannot reproduce traveling waves or sharp cell moving fronts [3]. Hence a modification by adding a new modeling term to the equations is necessary. The (K-S) model is also used in traffic flow modeling, where a nonlinear flux term in the equation can create unsteady or steady discontinuities (shock waves). So the idea here is to replace the (K-S) convection term $\nabla(a\rho\nabla c)$, where a is a constant, by

$$\nabla(f(\rho)\nabla c). \tag{2.1}$$

Let us consider a cell defined by a bounded domain $\Omega \subset \mathbb{R}^2$, and denote by $\rho(x,t)$ the cell density and $c(x,t)$ the concentration of some biochemical with the space and time variables $(x,t) \in \Omega \times [t_0, T],\ T > 0$. Thus the proposed model is written in the form

$$\begin{cases} \dfrac{\partial \rho}{\partial t} - \mu\Delta\rho + \nabla.(f(\rho)\nabla c) = r\rho\,(\rho_\infty - \rho) \quad on \quad \Omega \times [t_0, T], \\ \dfrac{\partial c}{\partial t} - \Delta c = s\left(\dfrac{\rho}{\rho_\infty} - c\right) \quad on \quad \Omega \times [t_0, T], \\ \rho(t_0) = \rho_0,\ c(t_0) = c_0 \quad on \quad \Omega, \end{cases} \tag{2.2}$$

where $\mu > 0$ is the diffusion rate, $\rho_\infty > 0$ is the threshold cell density and $f(\rho)$ is a nonlinear function from $[0, \infty[$ to $\mathbb{R}$.. The quantity c is the concentration of chemoattractant (or chemorepellent according to the sign of $f(\rho)$). The parameters $s > 0$ and $r > 0$ are a reaction rate for c and a proliferation rate for ρ, respectively.
In fact system (2.2) is used to model chemotaxis, where cells move towards higher concentrations of a chemical signal that they produce.

Logistic terms in (2.2)

1- Chemotactic Aggregation Term:
The term $\nabla.(f(\rho)\nabla c)$ in the first equation of (2.2) describes the movement of cells along the gradient of the chemical substance.

2- Source/Degradation:
In the first equation of (2.2), the term $\rho\,(\rho_\infty - \rho)$ in the right hand side represents the movement of cells. This term includes logistic growth (reproduction) and superlinear dampening (death).

3- Signal Production/Decay:
In the RHS of the second equation of (2.2), the term $\dfrac{\rho}{\rho_\infty} - c$, with $\dfrac{\rho}{\rho_\infty}$ representing production by cells, and

$-c$ represents natural decay.

The convective flux for the cells is

$$G = f(\rho)\nabla c. \tag{2.3}$$

The first constraint is $f(0) = 0$ (no flux i.e. no cell). In the direction $\eta = \frac{\nabla c}{\|\nabla c\|}$, there is a flux

$$g = G.\eta = f(\rho)\|\nabla c\| \tag{2.4}$$

The flux can be designed in order to attract cells located in low density regions toward denser regions (clustering) and to repel cells located in dense regions in order to colonize free regions (migration). One can consider for example a strictly concave function $f(\rho)$ such that $f(0) = 0$ and $f(\rho_c) = 0$ for some $\rho_c \in]0, \infty[$. We can consider for example a polynomial of degree 2 crossing the two points:

$$f(\rho) = \alpha\rho\left(1 - \frac{\rho}{\rho_c}\right) \tag{2.5}$$

with some constant $\alpha > 0$.

Description of the physical parameters

The physical parameters $\mu,\ s,\ r,\ \rho_c$ and ρ_∞ are described as follows:

***The diffusion rate** μ describes how fast particles spread from high to low concentration, , i.e. the measure of the change in the number of diffusing molecules inside the cell over time. This is calculated by Fick's Law as $(D \times A \times \Delta c)/\Delta x$, where D is the diffusion coefficient, A is the surface area, Δc is the concentration difference, and Δx is the distance.

***The migration rate** s is the measure of how many individuals move into or out of a population over a specified period.

***The prolifiration rate** r is the speed at which cells increase in number through growth and division, a critical process in development, tissue repair, and cancer, measured by tracking cell counts over time.

***The critical density** ρ_c in a cell context refers to specific thresholds in cell concentration or internal mass density (CMD) that trigger significant functional or structural changes.

***The threshold cell density** ρ_∞ refers to a critical concentration where cells trigger specific behaviors like communication, or shifts in metabolism.

In practice, they should be chosen according to some biological considerations and by identification from measurements.

Figure 1 shows the chemical flux (or chemotactic coefficient) as a function of the cell density ρ. Part (a) illustrates the region for $\rho \in [0, \rho_c]$ where the flux is positive, indicating movement towards the chemical gradient (attraction); while (b) characterises the region for $\rho \in [\rho_c, \rho_\infty]$ where the flux is negative, indicating movement away from the chemical gradient (repulsion). The vertical line at the critical density ρ_c clearly separates these two regions. This is a common characteristic in models of biological transport, such as cell migration in response to chemical signals, as clearly shown in Figure 1, where for $\rho \in [0, \rho_c]$, the flux is positive and the chemical species acts as a chemoattractant, while for $\rho \in [\rho_c, \rho_\infty]$, the flux is negative and the chemical species acts as a chemorepellent. Thus $f(\rho)$ in (2.5) is a suitable choice to be considered, in order to satisfy the requirements in section 2.1.

The characteristic velocity for the convective term is $v = f'(\rho)\nabla c$ leading to

$$v = \alpha \left(1 - 2\frac{\rho}{\rho_c}\right) \nabla c \tag{2.6}$$

There are two ways to get a null characteristic velocity leading to a locally stationary wave, either $f'(\rho) = 0$ or $\nabla c = 0$.

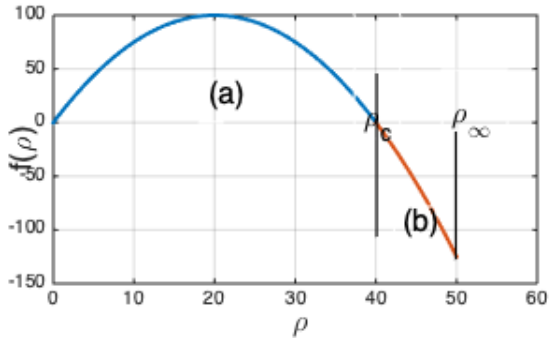

Figure 1: A plot of $(\rho \to f(\rho))$ for $f(\rho)$ in (2.5).

The well-posedness of mathematical models governing physical or biological phenomena is very important for a problem to be approximated numerically. Due to the french mathematician J. Hadamard at the beginning of the 19th century [9], a problem is well-posed if it has a unique solution that depends continuously on the initial data. This could be in the strong, mild or weak solution sense, depending on the considered partial differential equation and the given data.
Here we are first interested in proving the well-posedness of system (2.2) in the strong sens, using the semi-group theory [15] that is based on the famous Hille-Yosida theorem [5].

3. Well-posedness

In order to study the well posedness of (2.2), let us first establish some notations.
Let Ω be a bounded domain and $H = L^2(\Omega)$ equipped with the standard norm :

$$\|v\|_H = \left(\int_\Omega |v(\xi)|^2 d\xi\right)^{\frac{1}{2}} \quad ,$$

and $H^2(\Omega)$ the second order Sobolev space [1] defined by

$$H^2(\Omega) = \left\{v \in H : \partial^1 v \in H \quad and \quad \partial^2 v \in H\right\}$$

together with the norm

$$\|v\| = \left(\int_\Omega \sum_{k\leq 2} \partial^k v\right)^{\frac{1}{2}}$$

If we rewrite (2.2) in the form:

$$\begin{cases} \dfrac{dU}{dt} = AU + F(U). \\ U(x,0) = U_0. \end{cases} \tag{3.1}$$

with $U = (\rho, c)$. The operator A is defined on $D(A)$, where

$$A = \begin{bmatrix} A_1 & 0 \\ 0 & A_2 \end{bmatrix}; \quad A_1 = -\mu\Delta \quad and \quad A_2 = -\Delta + \nabla(f(\rho)\nabla) \tag{3.2}$$

$$F(U) = \begin{bmatrix} F_1(\rho) = r\rho(\rho_\infty - \rho) \\ F_2(c) = s\left(\dfrac{\rho}{\rho_\infty} - c\right) \end{bmatrix} \tag{3.3}$$

$$D(A) = \{U \in (H)^2, \, such \, that \, \nabla U|_{\partial\Omega} = 0\} \tag{3.4}$$

In the following, we introduce some important definitions and results needed in our study.

3.1. Reminders [15]

Let X be a Banach space and $D(A)$ a subspace in X.

Definition 3.1. A family of operators $(S(t))_{t\geq 0}$: $X \to X$ is a semi-group of linear operators on X if

- $S(0) = I$ (I is the identity operator on X),
- $S(t+s) = S(t)S(s)$ for every $t, s \geq 0$,

Moreover, it is C_0 semi-group if $S(t)x$ is continuous in $t \geq 0, \forall x \in X$ .i.e.,

$$\lim_{t\to 0} \|S(t)x - x\|_X = 0,$$

and when the norm of the C_0 semi-group satisfies

$$\|S(t)\| \leq 1,$$

it is called C_0 semi-group of **contrast** (for more details see [5] and [15]).

Definition 3.2. A linear operator $A : D(A) \subset X \to X$ is said to be **dissipative** if it satisfies:

$$\|(\lambda I - A)x\| \geq \lambda\|x\|, \ \forall\lambda > 0 \ \ and \ \forall x \in D(A).$$

It is called **m-dissipative (maximally dissipative)**, if it is dissipative and for all $\lambda > 0$, the operator $\lambda I - A$ is surjective, meaning that the range when applied to a domain D is the whole of the space X i.e. $(\lambda I - A = X)$.

Theorem 3.3. *(**Hille-Yosida Theorem** [5])*
A linear unbounded operator $(A, D(A))$ in X is the infenitisimal generator of a C_0 semi-group of contrast $(S(t))_{t\geq 0}$ if and only if A is m-dissipative with a dense domain in X.

In the following, we consider X to be a Hilbert space.

Theorem 3.4. *If A is m-dissipative, then $D(A)$ is dense in X [16].*

Theorem 3.5. *Let us consider the initial value problem :*

$$\begin{cases} \dfrac{du(t)}{dt} = Au(t) + F(u(t)); t \geq t_0, \\ u(t_0) = u_0, \end{cases} \tag{3.5}$$

where $A : D(A) \subset X \to X$. Let $F : [t_0, T] \times X \to X$ be continuous in t on $[t_0, T]$ and uniformly Lipschitz continuous (with a Lipschitz constant L) on X, i.e.: $\|F(u) - F(v)\| \leq L\|u - v\|, \ \forall u, v \in X$ and $L \geq 0$. If A is the infinitesimal generator of C_0 semi-group $(S(t))_{t\geq 0}$ on X then $\forall u_0 \in X$, (3.5) has a unique mild solution $u \in C([t_0, T]; X)$.
Moreover, the mapping $u_0 \to u$ is Lipschitz continuous from X into $C([t_0.T]; X)$ and the solution is expressed in the form :

$$u(t) = S(t - t_0)u_0 + \int_{t_0}^{t} S(t - s)F(s, u(s))ds. \tag{3.6}$$

For details on (3.6), the reader is referred to [16].

3.2. Application

Let us prove the well-posedness of ((3.1)-(3.3)), i.e. check the conditions of theorem 3.5. It is obvious that $F(U)$ defined by (3.3) is continous in $t \in (0,T)$

Let us prove that $F(U)$ is lipschitzian, starting by $F_1(\rho)$ defined in (3.3). Let $(\rho, c) \in H$, we write

$$\|F_1(\rho) - F_1(c)\| = \int_\Omega \left[r\rho(\rho_\infty - \rho) - rc(\rho_\infty - c)\right].$$

This results that

$$\|F_1(\rho) - F_1(c)\|_H \leq L \| (\rho - c) \|_H.$$

where $L = max\left(\sqrt{\sup_\Omega(f(\rho))}, \sqrt{r}\right)$. Similarly for $F_2(c)$ in (3.3), we get

$$\|F_2(\rho) - F_2(c)\| = \left(\int_\Omega [s(\frac{\rho}{\rho_\infty} - \rho) - s(\frac{\rho}{\rho_\infty} - c)]\right.$$

Thus

$$\|F_2(\rho) - F_2(c)\|_H \leq L^* \|(\rho - c)\|_H, \quad L^* = \sqrt{s}.$$

This proves that both F_1 and F_2 are lipchtzian. Hence F in (3.3) satisfies theorem 3.5 conditions.

Now we need to prove that A in (3.2) is the infinitesimal generator of C_0 semi-group $(S(t))_{t\geq 0}$ on H, i.e. show that A is dissipative and m-dissipative.

***Dissipativity of A**

We start by A_1

$$\begin{aligned}(A_1U, U) &= -\mu \int_\Omega \Delta\rho(x)\rho(x)dx. \\ &\leq \mu \int_\Omega (\nabla\rho(x)^2 dx + \int_{\partial\Omega} \nabla\rho(x)\rho(x)d\Gamma. \\ &\nabla\rho(x)|_{\partial\Omega} = 0. \\ &(A_1U, U) \leq 0 \; if \; \mu < 0.\end{aligned}$$

Identically for A_2, we have

$$\begin{aligned}(A_2U, U) &= \int_\Omega -\Delta\rho.\rho + \nabla(f(\rho)\nabla c).cdx. \\ &\leq \int_\Omega (1 + f(\rho))(\nabla\rho(x))^2 dx. \\ &(A_2U, U) \leq 0 \; if \; (f(\rho) < -1).\end{aligned}$$

Thus A is a dissipative operator.

***m-dissipativity of A**

To prove that $\forall F \in (H)^2, \forall \lambda \geq 0, \; \lambda U - AU = F$ has a unique solution i.e.

$$\lambda\rho - A_1\rho = F_1, \tag{3.7}$$

$$\lambda c - A_2 c = F_2, \tag{3.8}$$

we multiply equations (3.7) and (3.8) by v, w respectively, and integrate over Ω to get :

$$\lambda \int_\Omega \rho v dx + \mu \int_\Omega \nabla\rho.\nabla v dx = \int_\Omega F_1.v dx. \tag{3.9}$$

$$\lambda \int_\Omega c.w dx + \int_\Omega [\nabla c.\nabla w + f(\rho\nabla c).\nabla w dx] = \int_\Omega F_2.w dx. \tag{3.10}$$

Moreover if we write

$$a_1(\rho, v) = \lambda \int_\Omega \rho v dx + \mu \int_\Omega \nabla\rho\nabla v dx, \quad l_1(v) = \int_\Omega F_1 v dx,$$

$$a_2(c, w) = \lambda \int_\Omega cw dx + \int_\Omega [\nabla c.\nabla w + f(\rho\nabla c).\nabla w] dx, \quad l_2(w) = \int_\Omega F_2 w dx,$$

we can easily check the existence of a weak solution for ((3.9)-(3.10)), using Lax-Migram theorem [7, 10, 14]. Therefore A is m-dissipative.
As A verifies the conditions of theorem 3.3, then from theorem 3.5, we can say that problem ((3.1)-(3.3)) has a unique mild solution.

Let us now verify that U depends continuously on the initial data and that the mapping : $U_0 \to U$ is lipschitz and continuous.

Let W be a mild solution for ((3.7)-(3.8)),

$$\begin{aligned}\|U - W\| &\leq \|S(t - t_0)(U_0 - W_0)\| + \int_{t_0}^{t} \|S(t - t_0)\left[F(s, U(s)) - F(s, W(s))\right]\| dx, \\ &\leq B\|U_0 - W_0\| + BL \int_{t_0}^{t} \|F(s, U(s)) - F(s, W(s))\| dx,\end{aligned}$$

where B is a bound of $S(t)$ on $[t_0; t]$ and L is the Lipchitz-constant.

By using Gronwal theorem [5], we have

$$\|U - W\| \leq Be^{BL(t-t_0)}\|U_0 - W_0\|$$

which yields to the fact that U depends continuously on U_0 and $U_0 \to U$ is a Lipschitz continuous mapping.

3.3. Weak Formulation

If we multiply system ((3.1)-(3.3)) by (v, w), where v and w are the test functions for ρ and c respectively, and integrate over Ω, we get the following continuous weak formulation: Find $U = (\rho, c) \in (H^1(\Omega))^2$ such that $\forall(v, w)) \in (H^1(\Omega))^2$

$$\begin{cases} \displaystyle\int_\Omega \frac{\partial\rho}{\partial t}.v \; dx + \mu \int_\Omega (\nabla\rho\nabla.v) \, dx = \int_\Omega (F_1(\rho).v) dx, & (3.11) \\ \displaystyle\int_\Omega \frac{\partial c}{\partial t}.w \; dx + \int_\Omega (\nabla c.\nabla w + f(\rho).\nabla c.\nabla w) \, dx = \int_\Omega (F_2(c).w) dx, & (3.12) \end{cases}$$

where $F_1(\rho)$ and $F_2(c)$ are given in (3.3). Here $H^1(\Omega)$ is the standard Sobolev space. If we denote by $a(\rho, v)$ and $b(c, w)$ the bilinear forms and by $l_1(v)$ and $l_2(v)$ the linear forms, defined by:

$$a(\rho, v) = \mu \int_\Omega (\nabla\rho\nabla v) \, dx, \tag{3.13}$$

$$b(c, w) = \int_\Omega (\nabla c\nabla w + f(\rho)\nabla c.\nabla w) \, dx, \tag{3.14}$$

$$l_1(v) = \int_\Omega (F_1(c).v) dx, \tag{3.15}$$

$$l_2(w) = \int_\Omega (F_2(c).w) dx, \tag{3.16}$$

then the well-posedness of the weak formulation ((3.11) − (3.12)), i.e. the existence and uniqueness of a weak solution of (2.2) is proved by Lax-Miligram theorem based on the continuity and coecivity of the bilinear forms $a(.,.)$ in (3.13) and $b(.,.)$ in (3.14), together with the continuity of the linear forms $l_1(.)$ in (3.15) and $l_2(.)$ in (3.16). This is a straight forward task to check, see for example [5, 6] and [7].

3.4. Stability analysis

There are different methods for stability analysis, we can cite the two following :

- **Von-Neumann Method** : based on the decomposition of motion into normal modes, often using Fourier analysis, and superposition. The analysis looks at the growth or decay of perturbations from one step to the next one, and can be implemented using standard linear algebra procedures. A more severe restriction is that it applies only to linear systems, but despite this limitation, it can also be applied to linearised nonlinear systems [14].
- **Energy Methods:** well known as Lyapunov methods, where we look at the variation of certain function (or functional) measures of the motion amplitude [7]. Energy methods are not restricted to linear systems, but require the construction of suitable measures, usually related to energy.
  Here we use the energy method for the stability analysis of the derived system (2.2).

Let us now study the algebric stability of (2.2) by the energy method, assuming that $(r, s) << 1$ so that the right hand side of the first and second equations of (2.2) vanish. We multiply the first equation of (2.2) by ρ and integrate over Ω to get:

$$\begin{aligned}\frac{1}{2}\frac{d}{dt}\|\rho\|^2_{L^2(\Omega)} = \int_\Omega \frac{\partial \rho}{\partial t}\,\rho\,dx &= -\mu\int_\Omega \Delta\rho\,.\,\rho\,dx\\ &\leq max(\mu)\left(\int_\Omega (\nabla\rho)^2\right)dx\\ &\leq \psi\|\rho\|_{H^1(\Omega)}.\\ \frac{d}{dt}\|\rho\|_{L^2(\Omega)} &\leq 2\sqrt{\psi}\|\rho\|_{H^1(\Omega)},\ with\ \psi = max(\mu).\end{aligned}$$

In the same way, we multiply the second equation of (2.2) by c and integrate over Ω and get:

$$\begin{aligned}\frac{1}{2}\frac{d}{dt}\|c\|^2_{L^2(\Omega)} = \int_\Omega \frac{\partial c}{\partial t}\,c\,dx &= -\int_\Omega \Delta c\,c\,dx + \int_\Omega \nabla(f(\rho)\nabla c).c\,dx\\ &= \int_\Omega (\nabla c)^2 dx + \int_\Omega (f(\rho)\nabla c).\nabla c\,dx \leq \delta\int_\Omega (\nabla c)^2 dx\\ &\leq \delta\|\nabla c\|^2_{L^2(\Omega)}\\ \frac{d}{dt}\|c\|^2_{L^2(\Omega)} &\leq 2\delta\|c\|^2_{H^1(\Omega)},\end{aligned}$$

with $\delta = max(1, f(\rho))$.
Then we can deduce that the solution of (2.2) is stable in the energy sens.

4. Numerical Study

In this section, we develop a numerical scheme to solve system (2.2). We use a finite element scheme in space to discretise ((3.11)-(3.12)), following these steps:

- Chose a subspace $V_h \subset V = (H^1(\Omega))^2$, where $dim(V_h) = N < +\infty$,
- Construct a basis ϕ_h in V_h

- Compute the elements of the matrix κ_h and the vector b_h using the derived discrete weak formulations related to ((3.11)-(3.12)),
- Solve the resulting algebraic system $\kappa_h u_h = b_h$ for u_h,
- Finally find $U_h(x,y) = \Sigma u_h \phi_h$

For more details, see for example [2] and [5].

4.1. Numerical Discretisation

Let us consider a triangulation T_h of Ω, by using a numerical discretisation based on a finite element approach in space and an implicit scheme in time, i.e. Find $(\rho_h^{k+1}, c_h^{k+1}) \in (V_h)^2$ such that $\forall (v_h, w_h) \in (V_h)^2$ and given initial conditions $\rho_h^0 = \rho_0(x)$ and $c_h^0 = c_0(x)$, we get the following discrete system

$$\int_{T_h} \frac{\rho_h^{k+1} - \rho_h^k}{\Delta t}.v_h \; dx = \mu \int_{T_h} \left(\nabla \rho_h^{k+1}.\nabla v_h\right) dx + \int_{T_h} (F_1(\rho^{k+1}).v_h)dx, \tag{4.1}$$

$$\int_{T_h} \frac{c_h^{k+1} - c_h^k}{\Delta t}.w_h dx = \int_{T_h} \left(\nabla c_h^{k+1}.\nabla w_h\right) dx + \int_{T_h} f(\rho_h).\nabla c_h^{k+1} \nabla.w_h \; dx + \int_{T_h} (F_2(c^{k+1}).w_h)dx. \tag{4.2}$$

The discretisation parameters h and Δt are the space and time steps, respectively.
Note that the well posedness of the discrete system (4.1) and (4.2) is deduced from the well posedness of the continous (3.11) and (3.12).

For numerical stability analysis, it has to be pointed out that, it is observed that a standard CFL stability condition for explicit time-schemes (e.g. Euler) is very severe, and it is less than $\frac{1}{2}$ for semi-implicit schemes (e.g. Lax-Wendroff scheme). Here we use the implicit schemes $((4.1) - (4.2))$ which are unconditionally stable i.e the space and time discretisation parameters can be chosen adaptatively.
For the numerical experimentations, we follow the algorithm:

Algorithm 1

- Input: domain Ω, space discretisation parameter h, time step Δt, final time T, initial data ρ_0 and c_0, the physical parameters $s,\ r,\ \rho_c$ and ρ_∞, the diffusion rate μ and the constant α in (2.5)
For $t \leq T$,
- Compute: $U(x,t) = (\rho(x,t), c(x,t))$ from (4.1) and (4.2), using given initial conditions (ρ_0, c_0).

The related parameters $\mu,\ s,\ r,\ \rho_c,\ \rho_\infty$ defined and described in section 2.2, are adaptatively chosen from literature (see Table 1).

Table 1: Physical Parameters values

$\mu,\ s,\ r,\ \rho_c,\ \rho_\infty$		
Notation	**Value**	**Unit**
μ	10^{-2}	$(\mu m^2/s)$
s	10	$(cells/mL/h)$
r	0.01	$(mol/L.s)$
ρ_c	100	g/mL
ρ_∞	150	g/mL

The obtained numerical results are presented and discussed in the following section.

5. Results and discussions

For the numerical experimentations, the parameters are chosen as follows:

Discretisation parameters: h is set by an adapting meshing pocedure [14], as shown in Figures 2 and 3 (top left), i.e. we refine the meshing where it is needed in order to follow the motion of the cells and $\Delta t = 0.01$, here we use an implicit unconditionally stable scheme in time ((4.1)-(4.2)), maintaining the stability conditions in the energy sense, proved in section 3.4.

Physical parameters: are chosen adaptatively (see Table 1)).

Initial conditions: initial conditions are set as:

$$\begin{aligned} \rho_0 =& \rho_c[e^{-\beta(X_1^2+Y_1^2)} + e^{-\beta(X_2^2+Y_2^2)} + e^{-\beta(X_3^2+Y_3^2)}] \\ c_0 =& \rho_0/\rho_c, \end{aligned} \tag{5.1}$$

where $X_1 = x - Lx/4$, $Y_1 = y - Ly/2$, $X_2 = x - 3Lx/4$, $Y_2 = y - Ly/2$, $X_3 = x - 0.55Lx$ and $Y_3 = y - Ly/4$, with (Lx, Ly) the dimension of the domain Ω. Here β is a positive constant set to $\beta = 40$.
The open source PDE solver, using finite elements, software **FreeFem++ toolbox** [8] is employed for numerical solutions.
The results are resumed in Figures 2 & 3, where the densitiy and the concentration at different times t are visualised. The evolution of both is well apparent and the motion from uni-cellulars to more complex structure is achieved, highlighting a direct relationship between tumor growth and concentration of biochemical factors. We start with a system of three uni-cells and the evolution move to more complex structure formed from wave fronts. This shows that our satisfactory choice for $f(\rho)$ in (2.5) and visualised in Figure 1, meeting biological expectations as reported in section 2 and 3, yields these significant userful results. Furthermore, we can point out that the derived numerical scheme behaved in a stable manner and the obtained results show that cells move towards higher concentrations of the chemical signal, leading to a complex structure that is clear and uniform (see Figures 2 & 3).

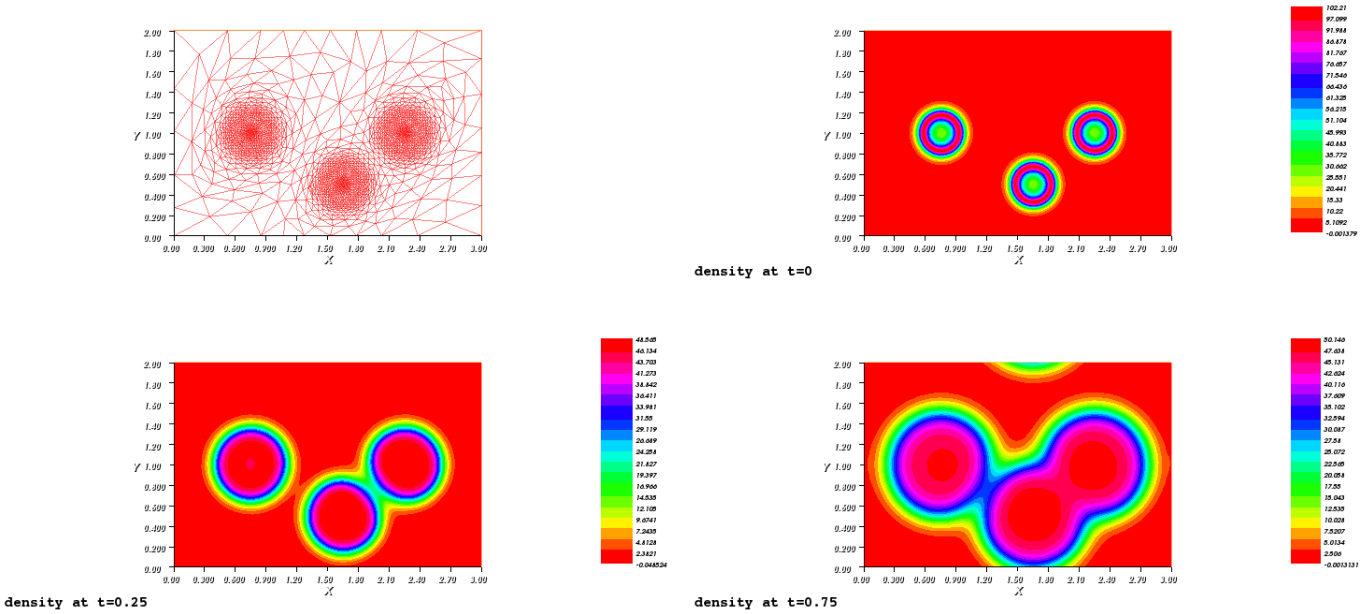

Figure 2: Density ρ_h solution of (4.1) for $t = 0,\ 0.25$ *and* 0.75.

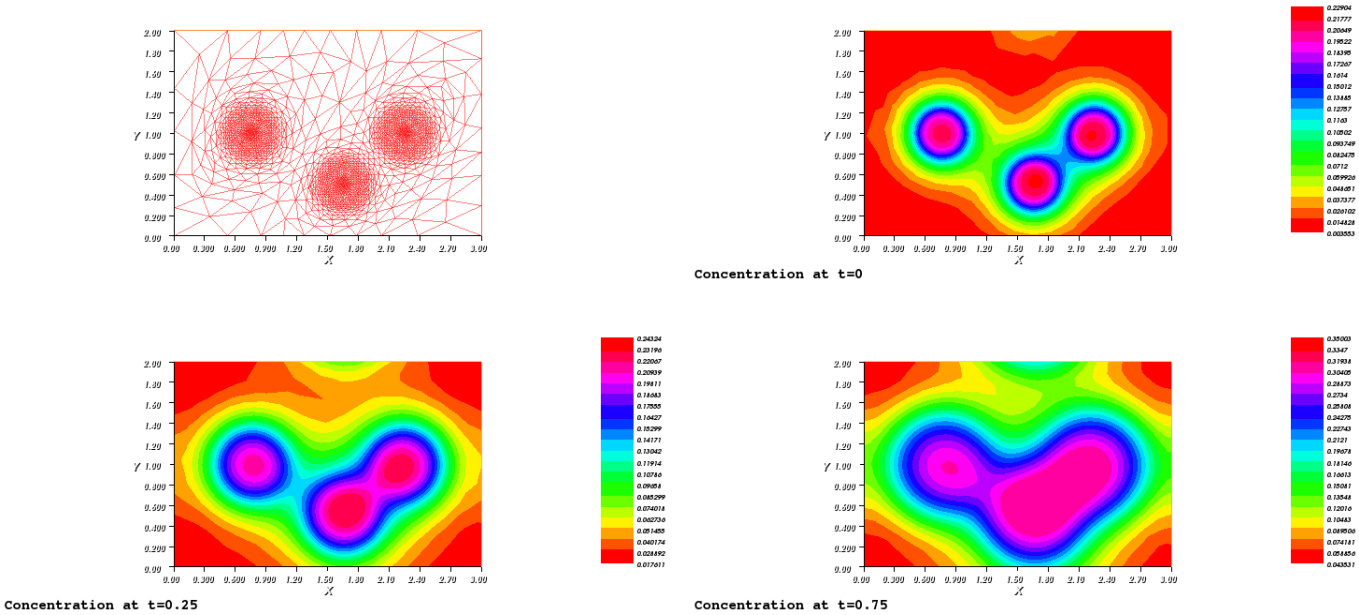

Figure 3: Concentration c_h solution of (4.2) for $t = 0,\ 0.25$ *and* 0.75.

6. Conclusion

A mathematical model based on the Keller-Segel system, able to fulfill biological requirements has been derived, when the cell density is large enough. Hence a modification by adding a new modeling term to the K-S equations was necessary, to understand how during the evolution of a tumor, the motion from a unicellular to more complex structure can be achieved, as shown in Figure 2. This is a common characteristic in models of biological transport, such as cell migration in response to chemical signals

The well-considered choice for $f(\rho)$ shown in Figure 1, satisfying biological expectations, is the main key of these obtained results

The well-posedness of the derived model is proved in the strong sense using semi-group theory, and in the weak sense by Lax-Miligram procedure. The numerical study has been carried out by the use of a stable numerical scheme based on finite elements in space with adaptation mesh and an implicit finite difference scheme in time that is unconditionally stable. The obtained numerical results are shown to be efficient and qualitatively significant for real biological applications. They highlight a direct relationship between concentration of biochemical factors and the density of tumor cells, confirming biological expectations underlined by the requirements in section 2.1, such that alive tumor cells perish in their absence, thereby promoting tumor growth, as shown in Figures 2 & 3.

It is essential to recognize that mathematical models serve as abstractions of biological processes, and their interpretation should be understood within the context of specific assumptions and model parameters. The complexity of biological systems manifests in the observed behavior, and a mathematical model may not precisely mirror the intricacies of actual biological phenomena. However, these results provide a valuable foundation for studying and potentially controlling tumor growth.

Validation against experimental data and consultation with experts in the field could provide further insights and confirmation in the field for an extension to models in 3D.

Aknowledgements: The authors are sincerely very grateful and thankful for the reviewers for their precious time, insightful feedback. Our deepest appreciation for their constructive comments, relevant remarks and their suggestions that improved this work.

References

[1] Adams, A.R., Fournier, J.J.F. (2003). Sobolev Spaces, 2nd ed. Elsevier Science Ltd. 3

[2] Allaire, G. (2005). Analyse numerique et optimisation. Une introduction à la modélisation mathématique et à la simulation numérique. Paris. 4

[3] Blanchet, A. (2010). A Gradient flow approach to Keller-Segel Systems. *https* : *//www.tse* − *fr.eu/sites/default/files/medias/doc/by/blanchet/dec*$_2$*010/b4.pdf*. 1, 2.2

[4] Brady, R., Enderling, H. (2019). Mathematical Models of Cancer: When to Predict Novel Therapies, and When Not to. Bull Math Biol, 81(12), 3722–3731. DOI: https://doi.org/10.1007/s11538-019-00640-x. 1

[5] Brezis, H. (2011). Functional Analysis, Sobolev Spaces and Partial Differential Equations. DOI : 10.1007/978-0-387-70914-7. 2.2, 3.1, 3.3, 3.2, 3.3, 4

[6] Meriem Boussebha and Fatma Zohra Nouri (2025), A Mathematical and Numerical Study of a Model for an Avascular Tumor Evolution, Dynamics of Continuous, Discrete and Impulsive Systems Series B: Applications & Algorithms 32, 247-267. 1, 2.1, 3.3

[7] N. Djedaidi, S. Gasmi and F.Z. Nouri (2023), Interface dynamics for a bi-phasic problem in heterogeneous porous media, Dynamics of Continuous, Discrete and Impulsive Systems Series B: Applications and Algorithms 30 (2023), pp. 21-33. 3.2, 3.3, 3.4

[8] https://freefem.org/Edition 2024 5

[9] Hadamard, J. (1952). Lectures on Cauchy's problem in linear partial differential equations. Dover, reprint. 2.2

[10] A. Hadji and F.Z. Nouri (2022), Mathematical and numerical study for a bioglass bioactivity degradation, International Journal of Advanced Science and Research , Vol 7, Issue 2, 2022, pp. 15-22. 1, 3.2

[11] Jones, D., Plank, M., Sleeman, B. (2009). Differential Equations and Mathematical Biology. New York: Chapman and Hall/CRC. *DOI* : *http* : *//doi.org*/10.1201/9781420083583. 1, 2.1

[12] Kolobov, A.V., Gubernov, V.V., Polezhaev, A.A. (2009). Autowaves in a model of invasive tumor growth. BIOPHYSICS, 54, 232–237. DOI: *https* : *//doi.org*/10.1134/*S*0006350909020195. 1

[13] Macias-Diaz, J.E., Gallegos, A. (2018). A structure-preserving computational method in the simulation of the dynamics of cancer growth with radiotherapy. J. Math Chem, 56, 1985–2000. DOI: https://doi.org/10.1007/s10910-017-0818-9. 1, 2.1

[14] F.Z. Nouri (2019), A New Approach for a Multiphase Flow Problem, Int. J. of Maths and Computation vol. 30 issue No 3, pp.32-42. 2.1, 3.2, 3.4, 5

[15] Pazy, A. (1992). Semi-groups of Linear Operators and Applications To Partial Differential Equations, 2nd ed. Springer-Verlag, Berlin-Heidelberg New York-Tokyo. 2.2, 3.1, 3.1

[16] Raymond, J.P. (n.d.). Evolution equation, University of Paul Sabatier. www.math.univ-toulouse.fr/ raymond/book-evolution.pdf. 3.4, 3.5

[17] Redouane, F., Jamshed, W., Devi, S.S.U. et al. (2022). Heat flow saturate of Ag/MgO-water hybrid nanofluid in heated trigonal enclosure with rotate cylindrical cavity by using Galerkin finite element. Sci Rep 12, 2302. https://doi.org/10.1038/s41598-022-06134-6 1

[18] Rejniak, K.A. (2007). An immersed boundary framework for modeling the growth of individual cells: an application to the early tumor development. J. Theor. Biol., 247(1), 186–204. 1, 2.1

[19] Rejniak, K.A. (2011). Hybrid models of tumor growth. Wiley Interdiscip. Rev. Syst. Biol. Med., 3(1), 115–125. 1

[20] Sabir, M., et al. (2017). A mathematical model of tumor hypoxia targeting in cancer treatment and its numerical simulation. Computers and Mathematics with Applications. DOI: http://dx.doi.org/10.1016/j.camwa.2017.08.019. 1

[21] Xu, J., Ding, L., Mei, J. et al. (2025) Dual roles and therapeutic targeting of tumor-associated macrophages in tumor microenvironments. Sig Transduct Target Ther 10, 268, 1-29. https://doi.org/10.1038/s41392-025-02325-5 1, 2.1